

## Convection Heat Transfer Coefficients for Laser Powder Bed Fusion

Mohammad Masoomi, Arash Soltani-Tehrani, Nima Shamsaei, Scott M. Thompson\*

Department of Mechanical Engineering, Auburn University, Auburn, AL 36849

National Center for Additive Manufacturing Excellence (NCAME), Auburn University, Auburn,  
AL 36849

*29th Annual International Solid Freeform Fabrication Symposium - An Additive Manufacturing  
Conference*

**August 2018**

### Abstract

This study investigates the effects of convection heat transfer during the laser-powder bed fusion (L-PBF) additive manufacturing process. For the L-PBF process, parts are fabricated under a purged, inert environment to avoid oxidation. Part of the delivered laser energy is transferred to the process chamber/environment through radiation and convection during fabrication. In this study, customized computational fluid dynamics (CFD) software is used to simulate the L-PBF of a single layer of stainless steel 17-4 PH. Local temperature and temperature gradients, as well as dimensionless numbers descriptive of important thermophysics, are provided in order to quantify local convective heat transfer. The results are used to predict local heat transfer coefficients during the L-PBF additive manufacturing process.

**KEYWORDS:** Laser powder bed fusion, Convective heat transfer coefficient,  
Temperature gradient, Numerical simulation

### 1. Introduction

Inert shielding gas is employed during welding and laser-based additive manufacturing (AM) processes to reduce oxide formation along part/powder surfaces, protect the melt pool against contamination and to aid in expelling so-called ‘spatter’ debris. Effects of shielding gas flow on welding/AM processes and on final material quality have been studied. Ly et al. [1] studied spatter generation during the laser-powder bed fusion (L-PBF) process via experimentation and it was shown that the presence of flowing argon gas can decrease spatter significantly relative to when the process is performed in vacuum. Wang et al. [2] studied the effects of shielding gas during laser deep penetration welding. It was shown that the shielding gas can help stabilize the laser welding process via convection heat transfer and enhanced ionization–recombination. Philo et al. [3] simulated the flow within an L-PBF (Renishaw AM 250) chamber. The flow atop the powder

\* corresponding author: [smthompson@auburn.edu](mailto:smthompson@auburn.edu)

bed was shown to be non-uniform and these flow non-uniformities increased spatter generation. Kah et al. [4] experimentally studied the effects of various shielding gases on the microstructure and mechanical properties of different materials including steel and aluminum during welding. For austenitic stainless steels, it was found that increasing the amount of nitrogen in the shielding gas can increase the ductility and improve the tensile strength, hardness, and pitting corrosion resistance of the final weld [4].

The L-PBF process may be numerically modeled and simulated using finite element (FE) methods [5]–[8]. Such approaches have been performed with varying degrees of fidelity for learning process-structure-property relationships while minimizing the need for repetitious, costly experimentation. In general, a continuum or powder-scale approach can be utilized, with the latter requiring significantly more computational resources. In order to produce realistic boundary conditions for performing more accurate laser-based AM simulations, the convection and radiation heat transfer along the surfaces of as-manufactured parts and surrounding powder should be appropriately considered.

In order to better represent boundary conditions, effects of convection need to be taken into account. Several different techniques and approaches have been used. In some cases, radiation and convection have been assumed as negligible during L-PBF [9]–[11], while others have assigned a uniform/constant heat transfer coefficient over all free surfaces. Peyre et al. [12] used a constant heat transfer coefficient of  $20 \text{ W/m}^2\cdot\text{°C}$ , Dong et al. [13] used  $25 \text{ W/m}^2\cdot\text{°C}$ , Espana et al. [14] used  $10 \text{ W/m}^2\cdot\text{°C}$ , while Denlinger et al. [15] and Parry et al. [16] used  $15 \text{ W/m}^2\cdot\text{°C}$ . Michaleris [7] assumed free convection around the powder bed and forced convection around the heat affected zone (HAZ), i.e.  $10 \text{ W/m}^2\cdot\text{°C}$  and  $21 \text{ W/m}^2\cdot\text{°C}$ , respectively. It was concluded that neglecting the effects of convection and radiation results in an over-prediction of temperature. More details on convection heat transfer modeling during L-PBF have been presented by Masoomi et al. [17].

The current study focuses on modeling the thermal response of a single track during typical L-PBF conditions while considering convection heat transfer with the inert shielding gas. The gas momentum and energy fields are found numerically while referencing temperature-dependent properties. Effects of convection and radiation heat transfer on the temperature distribution and temperature gradient of SS 17-4 PH during L-PBF are investigated. The difference between simulating L-PBF with an assumed constant heat transfer coefficient versus locally-variable heat transfer coefficients, found via CFD of surrounding fluid flow in the chamber, are also elucidated. Finally, data from simulations were used to propose a local heat transfer coefficient for the HAZ and rest of the build plate and results are compared to other simulations. In this study, effects of evaporation in the melt pool thermal response and its effects on convection have been neglected. Nonetheless, this study is believed to be a critical first step to understanding convection heat transfer due to shielding gas during L-PBF.

## **2. Physical model and numerical method**

The transient heat transfer during L-PBF of metals is complex; exhibiting dense heat flux transport, inhomogeneous phase change, small length/time scales, melt pool instability,

surface/fluid interaction, microstructural coupling, anisotropic microstructural growth and more [18], [19]. Utilizing a physical model that reduces this complexity can be advantageous for minimizing computational investment and for providing general insight into the process-property relationships inherent to parts fabricated via L-PBF. One such approach is to model the heat diffusion in all participating media while neglecting, or creatively accounting for, secondary/tertiary effects such as melt pool flow dynamics, powder bed mechanics, powder heterogeneity and microstructural evolution (i.e. solid-phase transformations). The melt pool, powder bed and solidified part can then be more readily modeled as continua with effective density and transport properties, and this approach is adopted herein. Melt pool advection and phase-change are accounted for by employing an effective melt pool thermal conductivity and in estimating latent heat transfer by computing solid/liquid phase fractions. Solid-phase nucleation, liquid-solid wetting phenomena, pore generation and the effect of powder size distribution are neglected. Effects of convection were modeled based on the technique presented by Masoomi et al. [17]. The shielding gas type was assumed to be argon with temperature-dependent properties.

### 3. Results and Discussion

Tetrahedral meshes were used for the powder bed and were uniformly dispersed at a size of  $\sim 3800 \mu\text{m}^3$  (mesh lengths of  $\sim 35 \mu\text{m}$ ). This mesh size was found to provide for mesh-independent results. The time step was chosen as 1 ms. Process parameters for fabrication of SS 17-4 PH are presented in Table 1. For all simulations the argon gas and laser were moving in the same direction.

**Table 1.** Process parameters for 17-4 PH stainless steel provided by EOS.

| Laser power (W) | Scan speed (mm/s) | Hatching distance ( $\mu\text{m}$ ) | Layer thickness ( $\mu\text{m}$ ) |
|-----------------|-------------------|-------------------------------------|-----------------------------------|
| 220             | 755.5             | 100                                 | 40                                |

Figure 1 presents the local temperature and temperature gradient response at the track's midpoint when the gas inside the chamber is modeled, Fig 1 (a), and when a constant heat transfer coefficient of  $20 \text{ W/m}^2\cdot\text{C}$ , is used. It may be seen that the maximum temperature of the melt pool drops around  $70 \text{ }^\circ\text{C}$  ( $\sim 3\%$ ) when the convection is calculated directly by modeling gas inside the chamber. This is due to a better prediction of convection and more accurate description of boundary conditions. This same trend is observed with the local, absolute temperature gradient. The temperature gradient is approximately 20% lower when the gas inside the chamber is modeled compared to the case where a constant heat transfer coefficient is used.

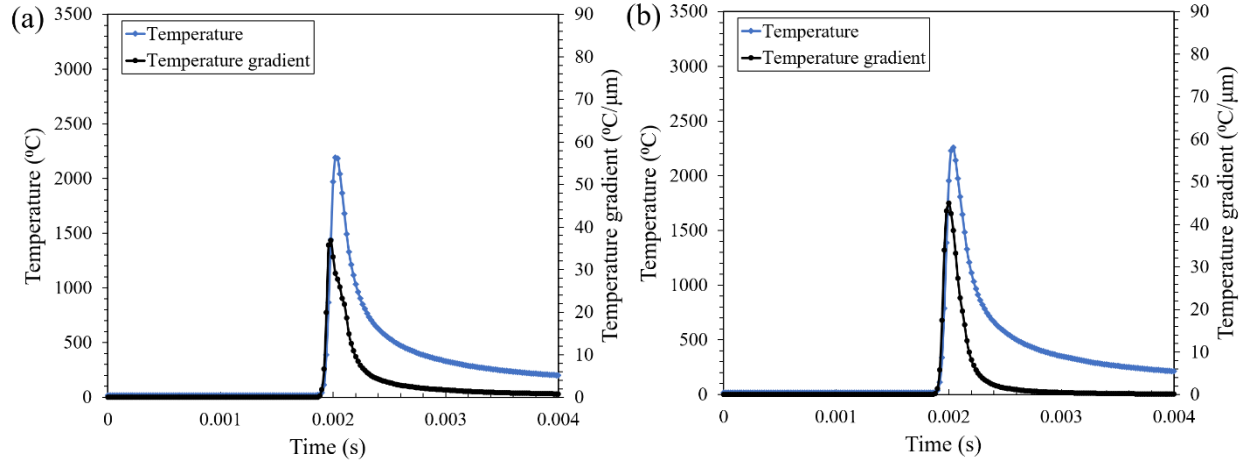


Figure 1. Temperature and temperature gradient at the middle of track when (a) convection is directly modelled in the chamber, (b) a constant heat transfer coefficient ( $h = 20 \text{ W/m}^2\cdot\text{°C}$ ) is used.

The Nusselt number is used to aid the characterization of convection heat transfer during the fabrication of parts, i.e. Eq. 1:

$$\text{Nu}_x = \frac{h_x x}{k_g} \quad (1)$$

where  $h_x$  is the local heat transfer coefficient and  $k_g$  is the thermal conductivity of the shielding gas. The local heat transfer coefficient was calculated using:

$$h_x = - \frac{k_g \left. \frac{\partial T}{\partial z} \right|_{z=0}}{(T_{s,x} - T_\infty)} \quad (2)$$

where  $T_{s,x}$  is the local surface temperature.

As shown in Fig. 2, the Nusselt number is higher near the HAZ during L-PBF. Based on the plot, and by using Eq. (2), the average heat transfer coefficient near the HAZ may be found to be  $\sim 1000 \text{ W/m}^2\cdot\text{°C}$  and for the rest of surface area at  $\sim 50 \text{ W/m}^2\cdot\text{°C}$ .

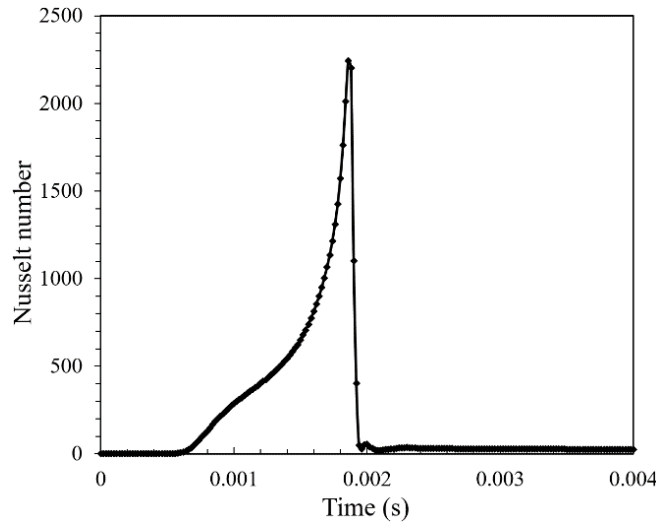


Figure 2. Nusselt number at the middle of track when convection is directly modelled in the chamber

Simulations were repeated by employing new heat transfer coefficients for the HAZ, at  $1000 \text{ W/m}^2\cdot\text{°C}$ , and rest of the area, at  $50 \text{ W/m}^2\cdot\text{°C}$ . The temperature and temperature gradient when using these modified heat transfer coefficients are presented in Fig. 3. It may be seen that by using the modified heat transfer coefficient, the accuracy for peak temperature increases by 2%. It may be seen that the maximum temperature changes by less than  $20 \text{ °C}$  when using the modified heat transfer coefficients. Additionally, the temperature gradient shows 10% improvement relative to using only a constant heat transfer coefficients. It is important to note that modeling the gas flow inside the chamber is computationally expensive and using modified heat transfer coefficients is more efficient.

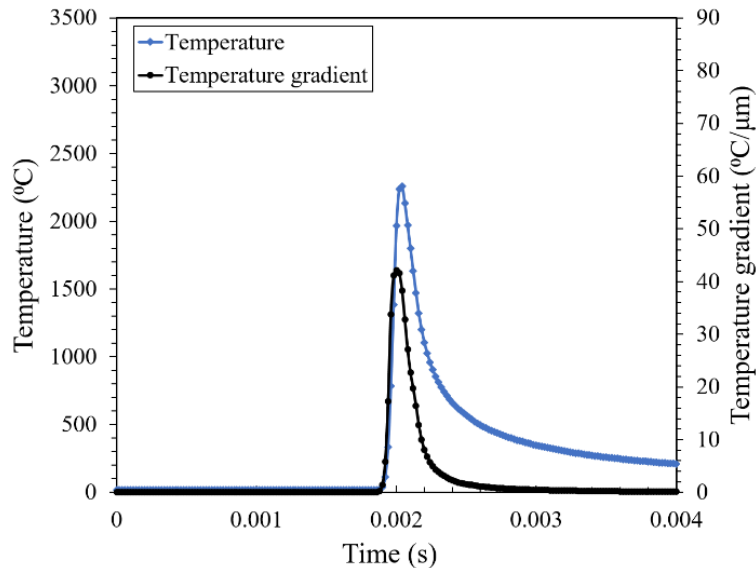


Figure 3. Temperature and temperature gradient at the middle of track when convection is directly modelled in the chamber

## 4. Conclusions

A continuum-based, numerical model was used to study the effects of shielding gas convection on total heat transfer during the L-PBF of SS 17-4 PH. The convective heat flux was calculated directly by modeling typical gas flow characteristics within the L-PBF chamber via computational fluid dynamics (CFD). The gas velocity and temperature boundary layers atop the powder bed and track were calculated. The combined melt pool/HAZ temperature distribution was found while either: (i) considering the gas-flow-coupled convective heat flux, (ii) constant heat transfer coefficient of  $h = 20 \text{ W/m}^2\cdot\text{°C}$ , or (iii) considering a modified heat transfer coefficient of  $h = 1000 \text{ W/m}^2\cdot\text{°C}$  for HAZ and  $h = 50 \text{ W/m}^2\cdot\text{°C}$  elsewhere. The major findings from the study are summarized below:

- 1) Modeling the gas inside the chamber will result in a more accurate prediction of thermal response during the L-PBF process compared to when using a constant heat transfer coefficient.
- 2) Convective heat transfer is more prominent near the HAZ compared to the rest of build area.
- 3) Using a modified heat transfer coefficient will improve the accuracy of thermal simulation compared to the case when a constant heat transfer coefficient is used.
- 4) The temperature gradient is more sensitive to convective heat transfer compared to maximum melt pool temperature.

Further studies can be done to better determine the effects of flow direction, gas speed and type of gas on convective heat transfer coefficients during L-PBF. A formula can be used to predict revised heat transfer coefficients based on the environmental conditions.

## 5. Acknowledgements

This work was partially supported by the National Science Foundation under Grant #1657195, and the National Aeronautics Space Administration (NASA) Grant #80MSFC17M0023.

## References

- [1] S. Ly, A. M. Rubenchik, S. A. Khairallah, G. Guss, and M. J. Matthews, “Metal vapor micro-jet controls material redistribution in laser powder bed fusion additive manufacturing,” *Sci. Rep.*, vol. 7, no. 1, p. 4085, Dec. 2017.
- [2] H. Wang, Y. Shi, S. Gong, and A. Duan, “Effect of assist gas flow on the gas shielding during laser deep penetration welding,” *J. Mater. Process. Technol.*, vol. 184, no. 1–3, pp. 379–385, Apr. 2007.
- [3] A. M. Philo, C. J. Sutcliffe, S. Sillars, J. Sienz, S. G. R. Brown, and N. P. Lavery, “A Study into the Effects of Gas Flow Inlet Design in a Renishaw AM250 Laser Powder Bed Fusion Machine Using Computational Modelling,” *Solid Free. Fabr.*, 2017.
- [4] P. Kah and J. Martikainen, “Influence of shielding gases in the welding of metals,” *Int. J. Adv. Manuf. Technol.*, vol. 64, no. 9–12, pp. 1411–1421, Feb. 2013.

- [5] Y. Li and D. Gu, "Parametric analysis of thermal behavior during selective laser melting additive manufacturing of aluminum alloy powder," *Mater. Des.*, vol. 63, pp. 856–867, 2014.
- [6] D. Riedlbauer, M. Drexler, D. Drummer, P. Steinmann, and J. Mergheim, "Modelling, simulation and experimental validation of heat transfer in selective laser melting of the polymeric material PA12," *Comput. Mater. Sci.*, vol. 93, pp. 239–248, 2014.
- [7] P. Michaleris, "Modeling metal deposition in heat transfer analyses of additive manufacturing processes," *Finite Elem. Anal. Des.*, vol. 86, pp. 51–60, Sep. 2014.
- [8] Y. Li and D. Gu, "Thermal behavior during selective laser melting of commercially pure titanium powder: Numerical simulation and experimental study," *Addit. Manuf.*, vol. 1–4, pp. 99–109, 2014.
- [9] H. Chung and S. Das, "Numerical modeling of scanning laser-induced melting, vaporization and resolidification in metals subjected to step heat flux input," *Int. J. Heat Mass Transf.*, vol. 47, no. 19–20, pp. 4153–4164, Sep. 2004.
- [10] M. Badrossamay and T. H. C. Childs, "Further studies in selective laser melting of stainless and tool steel powders," *Int. J. Mach. Tools Manuf.*, vol. 47, no. 5, pp. 779–784, Apr. 2007.
- [11] R. Paul, S. Anand, and F. Gerner, "Effect of thermal deformation on part errors in metal powder based additive manufacturing processes," *J. Manuf. Sci. Eng.*, vol. 136, no. 3, p. 31009, Mar. 2014.
- [12] P. Peyre, P. Aubry, R. Fabbro, R. Neveu, and A. Longuet, "Analytical and numerical modelling of the direct metal deposition laser process," *J. Phys. D. Appl. Phys.*, vol. 41, no. 2, p. 25403, 2008.
- [13] L. Dong, a. Makradi, S. Ahzi, and Y. Remond, "Three-dimensional transient finite element analysis of the selective laser sintering process," *J. Mater. Process. Technol.*, vol. 209, no. 2, pp. 700–706, 2009.
- [14] F. a. España, V. K. Balla, and A. Bandyopadhyay, "Laser surface modification of AISI 410 stainless steel with brass for enhanced thermal properties," *Surf. Coatings Technol.*, vol. 204, no. 15, pp. 2510–2517, 2010.
- [15] E. R. Denlinger, V. Jagdale, G. V Srinivasan, T. El-Wardany, and P. Michaleris, "Thermal modeling of Inconel 718 processed with powder bed fusion and experimental validation using in situ measurements," *Addit. Manuf.*, vol. 11, pp. 7–15, 2016.
- [16] L. Parry, I. A. Ashcroft, and R. D. Wildman, "Understanding the effect of laser scan strategy on residual stress in selective laser melting through thermo-mechanical simulation," *Addit. Manuf.*, vol. 12, pp. 1–15, 2016.
- [17] M. Masoomi, S. M. Thompson, N. Shamsaei, and J. Pegues, "A Numerical and Experimental Investigation of Convective Heat Transfer during Laser-Powder Bed Fusion," *Addit. Manuf.*, 2018.
- [18] Y. Huang, L. J. Yang, X. Z. Du, and Y. P. Yang, "Finite element analysis of thermal

behavior of metal powder during selective laser melting,” *Int. J. Therm. Sci.*, vol. 104, pp. 146–157, 2016.

- [19] Saad A. Khairallah Andrew T. Anderson Alexander Rubenchik, “Laser powder-bed fusion additive manufacturing: physics of complex melt flow and formation mechanisms of pores, spatter and denudation zone Saad,” *Igarss 2014*, vol. 108, no. 1, pp. 1–5, 2014.